



UNIVERSITY OF LEEDS

This is a repository copy of *Numerical investigation of the integration of heat transfer devices into a wind tower*.

White Rose Research Online URL for this paper:
<http://eprints.whiterose.ac.uk/81712/>

Version: Accepted Version

Proceedings Paper:

Calautit, JKS, Hughes, BR and Ghani, SA (2012) Numerical investigation of the integration of heat transfer devices into a wind tower. In: Proceedings of International Conference on Applied Energy. International Conference on Applied Energy, 5 - 8 July 2012, Suzhou, China. Applied Energy . (Unpublished)

Reuse

Unless indicated otherwise, fulltext items are protected by copyright with all rights reserved. The copyright exception in section 29 of the Copyright, Designs and Patents Act 1988 allows the making of a single copy solely for the purpose of non-commercial research or private study within the limits of fair dealing. The publisher or other rights-holder may allow further reproduction and re-use of this version - refer to the White Rose Research Online record for this item. Where records identify the publisher as the copyright holder, users can verify any specific terms of use on the publisher's website.

Takedown

If you consider content in White Rose Research Online to be in breach of UK law, please notify us by emailing eprints@whiterose.ac.uk including the URL of the record and the reason for the withdrawal request.



eprints@whiterose.ac.uk
<https://eprints.whiterose.ac.uk/>

NUMERICAL INVESTIGATION OF THE INTEGRATION OF HEAT TRANSFER DEVICES INTO A WIND TOWER

John Kaiser Calautit¹, Ben Richard Hughes¹, Saud Ghani²

¹ School of Civil Engineering, University of Leeds, Leeds, LS2 9JT, United Kingdom

² School of Mechanical Engineering, Qatar University, Doha, Qatar

ABSTRACT

Increasing focus on reducing energy consumption has raised public awareness of renewable energy resources, particularly the integration of natural ventilation devices in buildings such as wind tower systems. Wind towers have traditionally been used in Middle Eastern architecture for many centuries to provide natural ventilation and thermal comfort. The purpose of this study is to integrate heat transfer devices in a wind tower to meet the internal comfort criteria in extreme external conditions. Heat transfer devices were installed inside the passive terminal of the wind tower unit, highlighting the potential to achieve minimal restriction in the external air flow stream while ensuring maximum contact time, thus optimizing the cooling duty of the device. A geometrical representation of a full scale wind tower configuration, micro-climate and macro-climate was modeled. Computational Fluid Dynamics (CFD) was used to develop a numerical model of a new wind tower system and simulate the air flow pattern and pressure coefficients around and through the wind tower to the test room. Results have indicated that the average internal airflow rate was reduced following the integration of the vertical and horizontal heat transfer device configuration, reductions of 4.11 % and 8.21 % was obtained from the achieved numerical models. The work compared the effect of evaporative cooling and heat transfer devices on the thermal performance of the passive ventilation device. The proposed cooling system was capable of reducing the air temperatures by 12-15 K, depending on the configuration and operating conditions.

Keywords: wind tower, natural ventilation, passive cooling, CFD, heat transfer device

NONMENCLATURE

Abbreviation

CFD	Computational Fluid Dynamics
HTD	Heat Transfer Device
HVAC	Heating, Ventilation and Air-conditioning
WBCSD	World Business Council for Sustainable Development

Symbols

v	velocity [m/s]
---	----------------

p	static pressure [Pa]
T	Temperature [K]
\dot{m}	mass flow rate [kg/s]
g	gravitational acceleration (m/s^2)
u	x-direction velocity (m/s)
v	y-direction velocity (m/s)
w	z- direction velocity (m/s)
K	thermal conductivity (w/m-k)

Subscript

i	inlet
o	outlet
w	water injector
d	diffuser

1. INTRODUCTION

In hot and arid regions such as the Middle East, there is a large dependence on electricity to run mechanical systems for providing ventilation and thermal comfort. During the summer months more than 50 % of the electrical demand comes from HVAC loads [1-2]. As stated by WBCSD, commercial and residential buildings accounts for almost 40 % of the world energy usage and are responsible for almost 40-50 % of the world's carbon emissions. The resulting carbon emissions are substantially more than those in the transportation sector. This represents a significant opportunity for reducing the buildings energy consumption and green house gas emissions. Natural ventilative methods such as wind towers are increasingly being employed in new buildings to reduce the energy consumption and carbon foot print.

Wind towers have been in existence in various forms for centuries as a non mechanical means of providing indoor ventilation, energy prices and climate change agendas have refocused engineers and researchers on the low carbon credentials of modern equivalents. Conventional and modern wind towers architecture can be integrated into the designs of new buildings, to provide thermal comfort without the use of electrical energy.

A wind tower system is divided by partitions to create different shafts. One of the shafts functions as inlet to supply the wind and the other shafts works as outlet to extract the warm and stale air out of the living space as

shown in Figure 1. The temperature difference between the micro and macro climate creates different pressures and result in air currents. Experimental and numerical studies [3, 4] have shown that wind driven force is the primary driving force for the wind tower device, providing 76 % more indoor ventilation than buoyancy driven forces.

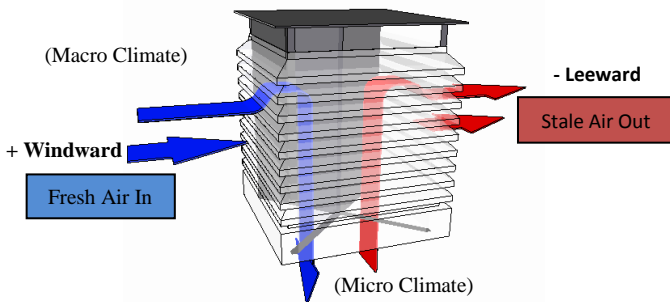


Figure 1 A flow diagram representing ventilation through a multi-direction wind tower device.

The cooling capabilities of wind towers which depend mainly on the structure design itself are inadequate. Therefore it is essential to cool the air in order to reduce the building heat load and improve the thermal comfort of its occupants during the summer months. Traditional wind tower systems were integrated with evaporative cooling devices to increase its thermal performance. The induced warm air is passed through cooling tubes or moist surfaces, which allows for the cooling of the air stream before entering the living spaces. However, the addition of these cooling devices may reduce the air flow rate inside the channel and reduce the overall efficiency of the wind tower. Another disadvantage of this configuration is the requirement of taller towers to have sufficient contact time between the air flow and cooling surfaces.

A wind tower system incorporating heat transfer devices was designed to meet the internal comfort criteria in hot and humid conditions. Heat transfer devices were installed inside the passive terminal of the wind tower unit, highlighting the potential to achieve minimal restriction in the external air flow stream while ensuring maximum contact time, thus optimising the cooling duty of the device. A numerical analysis was carried out using Computational Fluid Dynamics (CFD) software to simulate and analyze the air flow pattern, pressure coefficient and temperature distribution round and through the wind tower to the test room. The CFD commercial code used for the modeling of the wind tower is ANSYS Fluent. A geometrical representation of the wind tower configuration, micro climate and macro-climate was created using Solid Edge ST.

2. PREVIOUS RELATED WORK

Hughes *et al.* [5] highlighted the different cooling techniques integrated with wind tower systems to improve its thermal performance. Key parameters including the ventilation rates and temperature were evaluated in order to determine the viability of implementing the devices for their respective use. The results showed that the highest

temperature reductions were achieved from incorporating evaporative cooling techniques into the wind tower such as wetted column (clay conduits) and wetted surface (cooling pads). The temperature reduction was found to be in the range of 12 –15 K. The study also highlighted the effect of the addition of the cooling devices inside the device which reduces the air flow rates and reduces the overall efficiency of the wind tower.

Kalantar [6] assessed the ventilation and thermal performance of a traditional wind tower located in the hot and arid region of Yazd. The work developed a numerical CFD model to simulate and analyze the airflow pattern inside the wind tower in three-dimensional and steady state conditions. The study also presents a numerical technique to simulate the effect of integrating evaporative cooling systems to the wind towers performance. The result yielded a good correlation between the numerical simulations and experimental data obtained from literature. It was found that the Badgir wind tower was able to reduce the air temperatures by 10 to 15 K

Bouchahm *et al.* [7] evaluated the ventilation and thermal performance of a similar wind tower system incorporated to a building using experimental and theoretical methods of analysis. Clay conduits were mounted inside the shaft of the unidirectional tower to improve the mass and heat transfer and a water pool is situated at the bottom of the device to increase the humidification process. The results confirmed that the airflow induced by the 0.75 x 0.70 m² tower has a direct effect on the reduction of internal temperature. It was found that small sized partitions (by increasing the number of conduits) better efficiency is achieved than with a higher wetted column of the cooling tower. The cooling tower integrated with wetted interior surfaces was able to reduce the indoor air temperature by up to 17.6 K.

Badran [8] investigated the performance of an evaporative cooling and multi-directional wind tower system. A mathematical model was developed to analyze the condition of air passing through the evaporative cooling column of the tower for different external conditions. Similarly, clay conduits were installed inside the tower's channel to cool the passing airflow before inducing it inside the structure. During the night, the ambient air coolness is stored in the conduits mass to let it function during the day. The results showed that the evaporative cooling tower with a vertical height of 4m can generate an airflow of 0.3 m³/s and reduce the internal temperature by 11 K. The author suggested that reducing the height of the wind tower which generally reaches up to 15 m can decrease the construction cost without having a noticeable decrease in performance.

Safari and Hosseinnia [9] used analytical and numerical CFD modeling to investigate the thermal performance of new designs of wind towers under different structural parameters and external conditions. The novel wind tower

design is equipped with wetted curtains suspended inside the column of the cooling device, which are formed as surfaces that inject droplets of water at extremely low speeds. The achieved numerical results showed that the wetted columns with the height of 10 meters were able to reduce the internal air temperature by 12 K and increase the relative humidity of air by 22 %.

From the previous related work, different types of wind tower cooling methods have been studied using numerical CFD analysis. Furthermore, several works have also used analytical methods and far-field testing to validate the results. The role of each parameter to the overall efficiency of the wind tower system is established and presented. The numerical simulation and experimental results demonstrated the importance of the use of CFD in assessing the performance of a wind tower system. The good correlation between both methods of analysis suggests that the CFD techniques in use were suitable for this type of device and such have been used for the purpose of this research.

The study evaluates the performance of the proposed model by simulating and analyzing the air movement and temperature in the structure using CFD, highlighting the potential to achieve minimal restriction in the external air flow stream while ensuring maximum contact time. The numerical solutions are validated against experimental and computational data obtained from literature [4, 6]. The level of performance of the design is assessed based on the results of the internal air velocity, pressure and temperatures.

3. CFD SET-UP

The CFD analysis was carried out using the ANSYS 12.1 Fluent software. The CAD model was imported to Workbench: Model Designer to generate a computational model. The geometrical model of a wind tower channel with a height of 10 m and $1.5 \times 1.5 \text{ m}^2$ cross-sections is used to compare the performance of a passive system incorporating evaporative cooling and heat transfer devices. A water injection system for the cooling of the air stream is located at the top of the wind tower channel ($h = 9\text{m}$).

Figure 2 shows a three-dimensional drawing of the computational model and the location of the measurement points inside wind tower channel along with their dimensions.

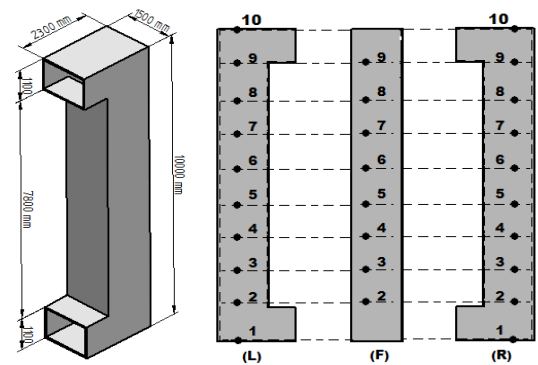


Figure 2 Schematic of the wind tower channel and positioning of the sample points (Stage 1)

Furthermore, the wind tower system with evaporative cooling and heat transfer devices are incorporated to a test room (micro climate) with the height, width, and length of 3, 6, and 6 m. An enclosure was created to represent the external wind environment (macro climate). The enclosure with a height, width, and length of 8, 26, and 46 m creates a direct interface through the geometry. The air streamline had a constant velocity of 3 m/s through the enclosure to simulate the actual wind environment. The enclosure (the flow domain) was set at a distance from the geometry to avoid reversed flow in the region [10]. A flow domain representation of the physical geometry of the wind tower design under investigation and location of set boundary conditions are shown in Figure 3.

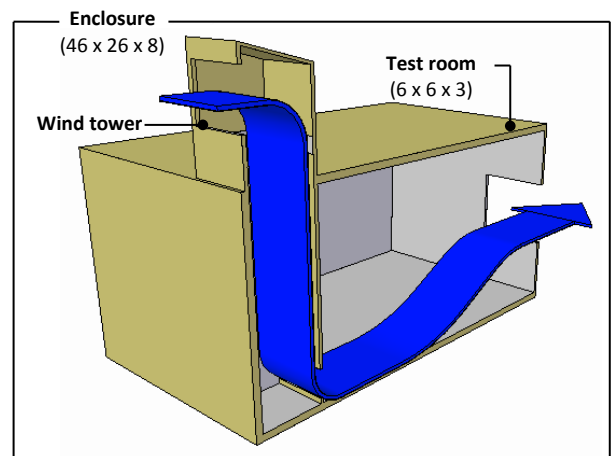


Figure 3 Schematic of a wind tower system mounted on the test room (Stage 2)

A four-sided square wind tower with an internal diameter of 1 m and height of 1.5 m is used for the numerical analysis. The vertical HTD arrangement is identical to the standard wind tower model, the heat transfer devices are closely arranged in an x-shaped vertical pattern positioned next to the cross-dividers inside the passive terminal. A one-sided circular wind tower is used for the analysis of the horizontal heat pipe configuration, while retaining the physical parameter and standard components of the benchmark model. Figure 4 displays the proposed configurations.

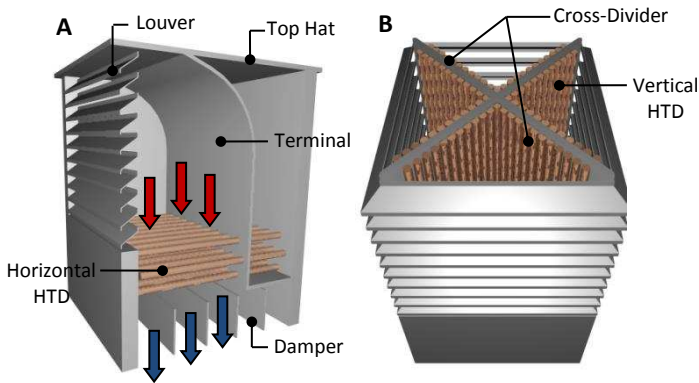


Figure 4 Wind tower systems incorporating (a) horizontal HTD arrangement (b) vertical HTD arrangement

Table 1 displays the design specification of the heat transfer devices employed in the wind tower system. Table 2 summarizes the conditions of the test configurations.

Table 1 Design Specification of HTD arrangements

Specification	Vertical	Horizontal
Number of Heat Transfer Device	70	70
Spacing (m)	100	100
Pitch Spacing (m)	100	100
Outer Diameter (m)	20	20
Inner Diameter (m)	15	15
Length (m)	900	900

Table 2 Summary of the wind tower test configurations

Test	Wind Direction	Wind Speed	Wind Tower Type	Cooling Device
1	0°	0-5	One-sided	Evaporative
2	0°	0-5	Four-sided	N/A
3	0°	0-5	Four-sided	Vertical HTD
4	0°	0-5	One-sided	Horizontal HTD

3.1 Mesh Generation

The quality of the mesh has important implication on the convergence and the level of accuracy of the achieved results [11]. The size of the mesh element was extended smoothly to resolve the sections with high gradient mesh and to improve the accuracy of the results of the temperature fields, as shown in Figure 5.

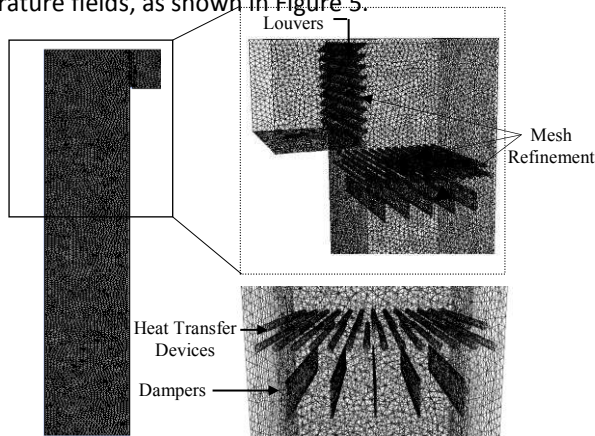


Figure 5 Schematic diagram representing the wind tower channel with grid sections.

A non-uniform mesh was applied to the volumes of the computational model. The mesh arrangement consisted of 344,643 non-uniform mesh elements with 70,435 nodes, as shown in Figure 6.

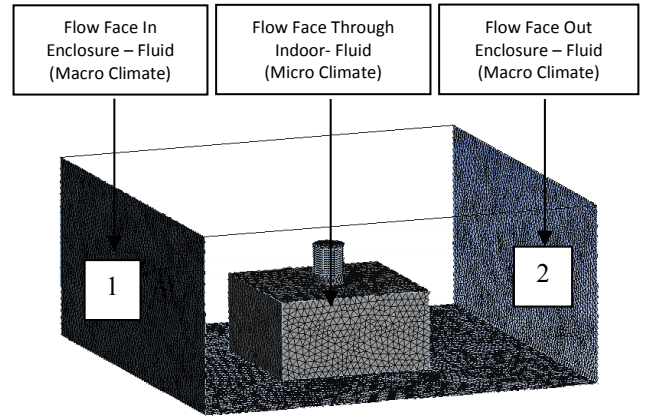


Figure 6 Flow domain representation of the physical geometry of the wind tower design under investigation and location of set boundary conditions.

3.2 Boundary conditions

The k -epsilon(2eqn) viscous model with standard wall functions was used for the numerical simulation as it is the most appropriate viscous model for an inlet wind velocity of 4 m/s and lower [11]. The obtained CFD results of the wind tower system incorporating evaporative cooling methods will be validated against research carried out by Kalantar [6] on a wind tower channel by using both analytical and CFD analysis. A similar geometrical structure, boundary conditions and CFD codes were applied. Figure 7 displays the computational domain of the traditional and modern design of a wind tower system integrated with cooling devices. Evaporative cooling devices sit at the top of a wind tower. Hot air is passed through the wind tower channel and cooled by the water evaporation. Cool moist air is denser than ambient air and sinks down the tower and into the enclosed space [12]. Computational model of the wind tower channel incorporating cooling devices with boundary conditions are summarized in Figure 7.

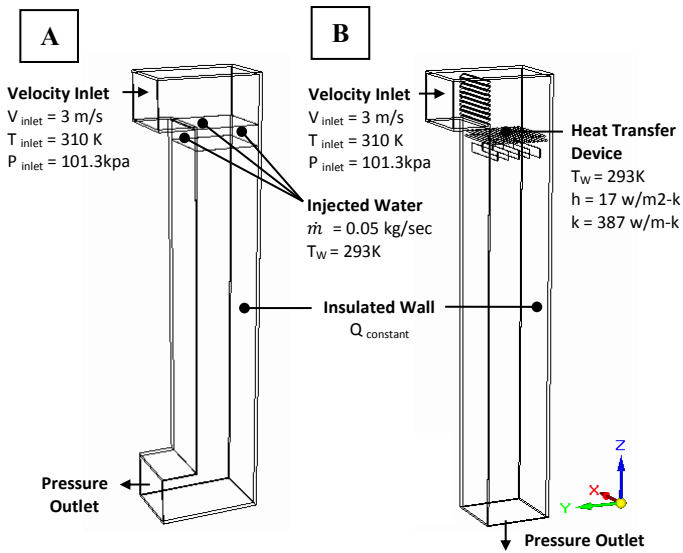


Figure 7 Computational domain with boundary conditions: (a)traditional evaporative cooling (b) HTD

The geometry (micro climate) was modelled as an open structure with openings on the windward and leeward side which allows the incoming air to pass through it, in order to simulate and analyse the air flow pattern inside the structure. The geometry faces were set as solid walls with a thickness of 0.2 and 0.02 m to create a boundary between the interior and exterior.

The enclosure (macroclimate) was created to simulate the external wind velocity. The enclosure consists of a velocity inlet (operating velocity) at the left hand side of the enclosure, and a pressure outlet (atmospheric pressure) on the opposing boundary wall of the enclosure as shown in Figure 8.

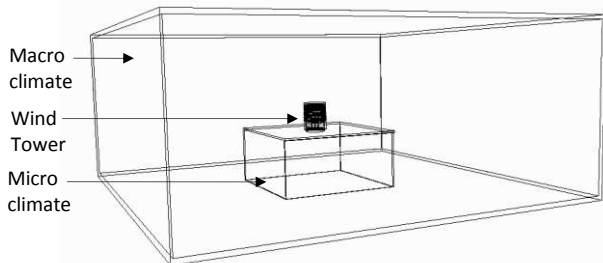


Figure 8 CFD flow domain representation of the micro and macro climate environment (Stage 2).

The base of the structure is set as ground (wall) and the remaining faces were set as symmetry to alleviate any return velocities which could affect the precision of the results. The boundary conditions for the CFD model are shown in Table 3.

Table 3 CFD Model Boundary Conditions

Geometry	Solid
Mirco-Macro climate	Fluid (air)
Ground	Wall
Velocity inlet (m/s)	5, 4, 3, 2, 1
Pressure outlet	Atmospheric

Viscous model	k-epsilon (eqn (2))
Near-Wall treatment	Standard Function
Velocity formulation	Absolute
Time	Steady State
Gravity	-9.81 (Z-Axis)
Test Room wall Thickness(m)	0.2
Wind Tower Wall Thickness(m)	0.02
External Temperature (K)	310
Heat Transfer Coeff. (W/mK)	8.9

3.3 Grid adaption

Grid adaptation was used to validate the programming and computational operation of the computational model. The numerical grid was refined and locally enriched using the hp-method grid adaptation technique [13]. This procedure of evaluation requires the use of different mesh sizes or higher order approximations by the use of a posterior error estimates. The posteriori error estimate used in the theoretical model is the average weighted velocity taken from the interior (micro climate) of the test room. Also, due to the complexity of the geometry the mesh was generated using tetrahedral elements with patch conforming algorithm. The grid adaptation procedure increases the number of nodes and elements of the numerical model. The grid was evaluated and refined until the posterior estimate error becomes insignificant between the number of nodes and elements, computational iterations and the posterior error indicator [11]. The applied boundary conditions were remained fixed throughout the simulation process to ascertain precise comparison of the posterior error estimate. Results are shown in Table 4.

Table 4 Grid adaption for verification of CFD model

No. of Nodes	70,435	89,464	143,161	247,080
No. of Elements	344,643	435,488	713,837	1,401,913
Relevance Centre	Coarse	Coarse	Coarse	Coarse
Element Size	0.6	0.5	0.4	0.3
Mesh Matrix	Tet	Tet	Tet	Tet
Velocity Inlet(m/s)	2.05	1.94	1.93	1.93
Velocity Outlet (m/s)	0.61	0.60	0.61	0.61
Velocity Indoor (m/s)	0.85	0.80	0.79	0.78
Velocity Diffuser (m/s)	1.85	1.80	1.72	1.70

Figure 9 shows that at 1,400,000 elements the percentage error between the grid refinements was at its lowest in the last two steps. An acceptable compromise was reached between the accuracy of results and computational iterations. The variables are the average velocity at the inlet and outlet of the wind towers and interior of the test room

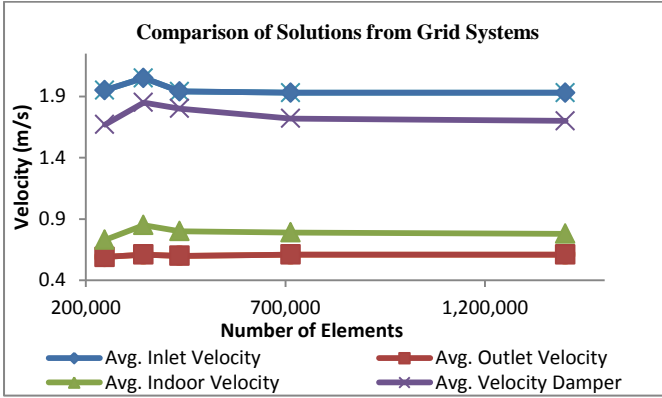


Figure 9 The solutions using various grid adaptation methods. The variables are the average velocity at the inlet and outlet of the wind towers and interior of the test room

4. RESULTS

Figure 10a displays the velocity contour of the cross-sectional plane inside the evaporative cooling tower test channel. The increase in velocity is due to absorption of water by the air and it is in a heavier state (denser). Figure 10b shows that the velocity is accelerated as it moves across the 35° louvers, reaching a maximum velocity of 3.5 m/s. It is also observed that the velocity increases in the upper turns of the wind tower as the cross-section of the air flow decreases due to the vortex formation [14]. As can be seen from Figure 11, the CFD results in this study [6] are comparable (range 0-11 % error)

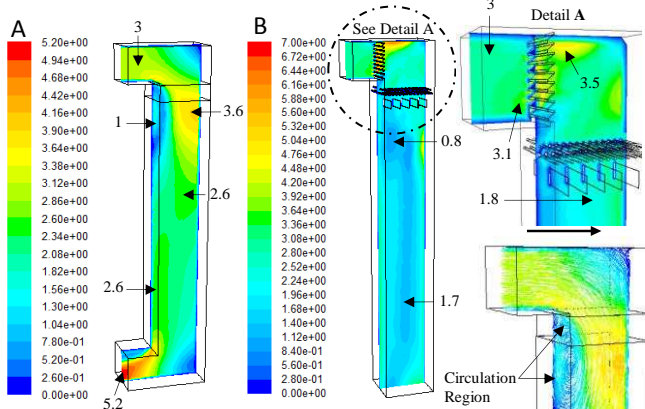


Figure 10 Velocity contour lines of a cross sectional plane in the test channel: (a) evaporative cooling (b) HTD

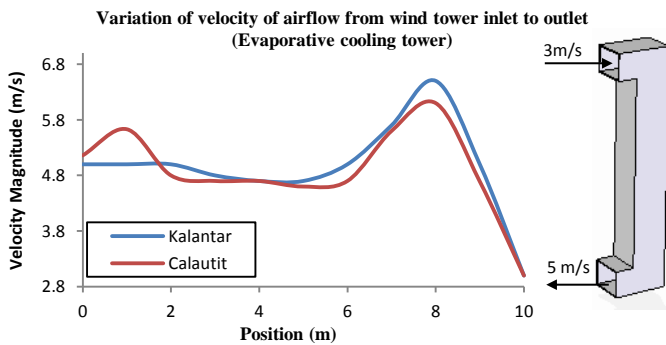


Figure 11 Comparison of the airflow velocity obtained from the CFD data from the two studies.

Figure 12a shows the contours of static temperatures inside the modified test channel. From the illustration it is seen

that there is a sufficient decrease in air temperature. This is due to the absorption of heat in the evaporative cooling. The water is sprayed at the top section of the channel ($h=9$ m), temperature decrease very fast and slightly increases due to the walls of the wind tower. From Figure 12b, the temperature reduction is greater on the left side of the contour plot where the air velocity is lower (see Figure 10b). This is due to the increase in contact time between the HTD and air. As can be seen from Figure 13, the CFD results in this study [6] are comparable (range 0-0.5 % error)

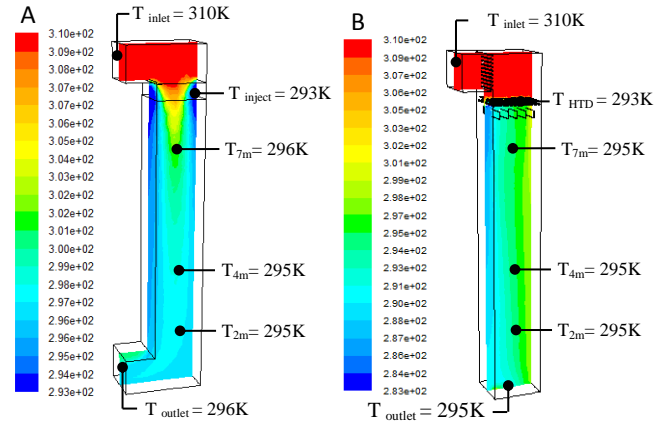


Figure 12 Temperature contour lines of a cross sectional plane in the test channel: (a) evaporative cooling (b) HTD

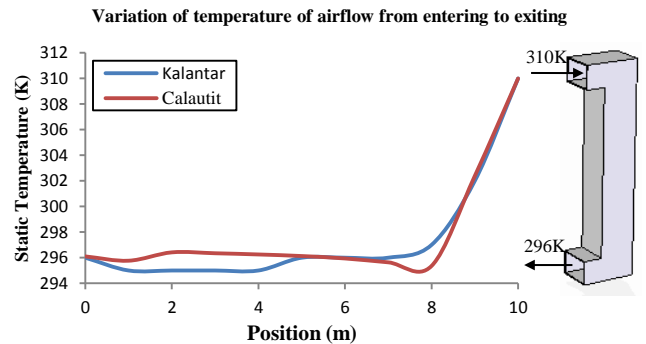


Figure 13 Comparison of the airflow temperature obtained from the CFD results from the two studies.

Figure 14 compares the thermal performance of a wind tower system incorporated with evaporative cooling and HTD.

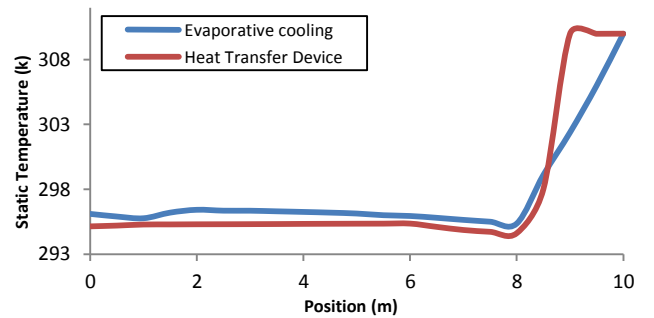


Figure 14 Comparison of the variation of temperature of airflow from entering to exiting.

Figure 15 displays the effect of the vertical wind tower height on the thermal performance. It can be observed that

the traditional system is greatly dependent on the height of the tower.

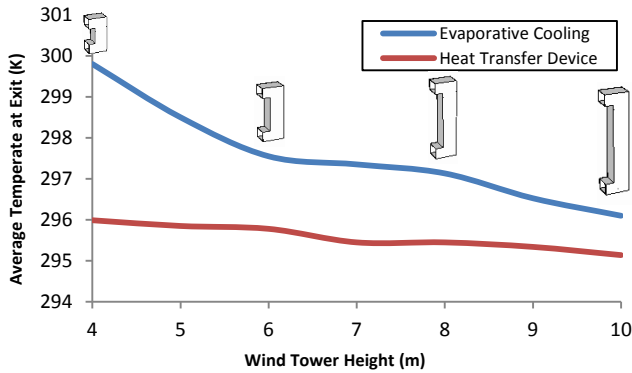


Figure 15 Effect of the wind tower height on the temperature at exit.

Figure 16 display the velocity contour of the cross-sectional plane in the test room model. From the illustration it is observed that the air flow entering the opening of the uni-directional wind tower is directed down to the enclosed space through the floor diffuser. The airflow is accelerated as it shears across the walls and floor of the structure, reaching a maximum velocity of 3 m/s.

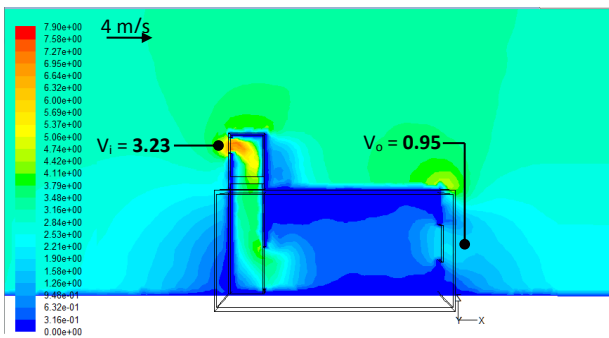


Figure 16 Velocity contour lines of a cross sectional plane in the test room with an inlet velocity of 4 m/s (Evaporative cooling)

Figure 17 shows the contours of static temperatures inside the test room. From the illustration it is seen that there is a sufficient decrease in air temperature, reductions of 13 K is obtained.



Figure 17 Temperature distributions within the test room with external wind speeds of 4 m/s (Evaporative cooling)

Tables 5 summarize the CFD results for the simulated velocity and pressure regions for the traditional tower.

Table 5 Numerical CFD results (Evaporative cooling)

External wind (m/s)	V_{indoor} (m/s)	V_i (m/s)	V_o (m/s)	P_i (Pa)	P_o (Pa)
1	0.29	0.92	0.35	0.99	-0.42
2	0.47	1.58	0.58	3.72	-3.19
3	0.68	2.39	0.86	5.56	-5.09
4	0.86	3.23	0.95	8.24	-7.84
5	1.01	3.71	1.21	10.21	-8.78

The modern wind tower was located centrally within the micro climate. The position of the measuring points inside the test room is shown in Figure 18. The center of the wind tower was located directly above sample point 5. The vertical distance at which the sample points were taken was 1.5 m with the additional point taken at 2.75 m (diffuser level).

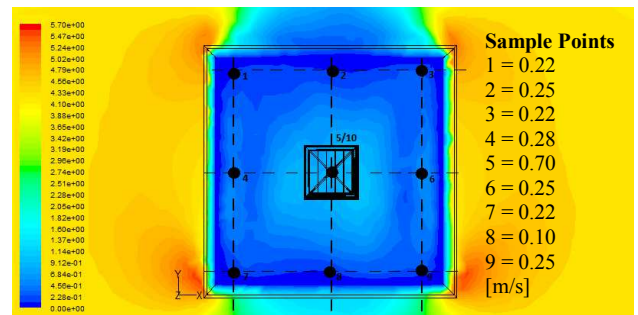


Figure 18 Contour plot of internal velocity at external velocity of 4 m/s showing the location of sample points within the microclimate (Modern wind tower).

Figure 19 shows the pressure distribution at a cross-sectional plane passing through the centre of the ventilation device. From the illustration, it is observed that the areas of high pressure are observed at the wind ward side of the tower. While low pressure areas are seen inside the microclimate and at the outlet of the wind tower

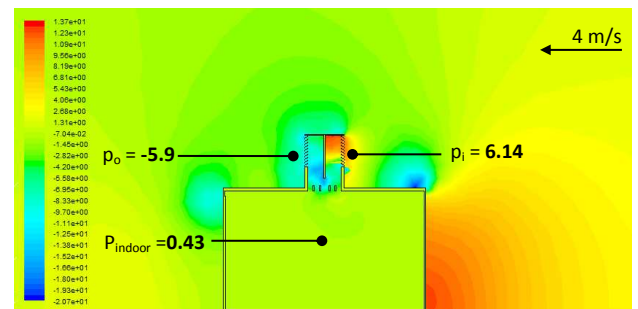


Figure 19 Static pressure contour plot of a cross sectional plane in the test room with an inlet velocity of 4m/s (Modern wind tower)

Tables 6, 7 and 8 summarize the CFD calculated results for the simulated velocity (1, 2, 3, 4 and 5 m/s) and pressure regions for the benchmark model, vertical heat pipe configuration, and horizontal heat pipe configuration. Results have indicated that the internal airflow rate was slightly reduced following the integration of the vertical and heat pipe configuration, reductions of 4.11 % and 8.21 % was obtained from the achieved computational model.

Table 6 Numerical CFD results (Modern wind tower)

External wind (m/s)	V_{indoor} (m/s)	V_i (m/s)	V_o (m/s)	V_d (m/s)	P_i (Pa)	P_o (Pa)
1	0.17	0.47	0.15	0.47	0.54	-0.32
2	0.39	0.96	0.28	0.94	1.89	-1.19
3	0.55	1.45	0.44	1.29	3.73	-3.07
4	0.73	1.95	0.59	1.67	6.14	-5.88
5	0.85	2.25	0.64	1.82	7.84	-6.71

Table 7 Numerical CFD results (Vertical HTD Arrangement)

External wind(m/s)	V_{indoor} (m/s)	V_i (m/s)	V_o (m/s)	V_d (m/s)	P_i (Pa)	P_o (Pa)
1	0.16	0.34	0.20	0.45	0.53	-0.19
2	0.36	0.73	0.37	0.89	1.80	-0.79
3	0.53	1.13	0.49	1.29	3.55	-1.83
4	0.70	1.52	0.60	1.67	5.55	-3.39
5	0.82	1.67	0.72	1.91	6.57	-4.78

Table 8 Numerical CFD results (Horizontal HTD Arrangement)

External wind (m/s)	V_{indoor} (m/s)	V_i (m/s)	V_o (m/s)	V_d (m/s)	P_i (Pa)	P_o (Pa)
1	0.14	0.45	0.23	0.41	0.64	-0.55
2	0.37	0.91	0.57	0.77	2.04	-2.12
3	0.52	1.35	0.81	1.12	3.96	-4.39
4	0.67	1.79	1.08	1.47	6.43	-7.57
5	0.75	1.89	1.15	1.67	7.41	-9.21

Figure 20 illustrates temperature distribution inside the test room integrated with a modern wind tower device. It is observed that the temperature is reduced as it approaches the cross-dividers with the vertical HTD arrangement. The average temperatures inside the microclimate are 296.2 K and 295.8 K with the macro climate temperature set at 310 K.

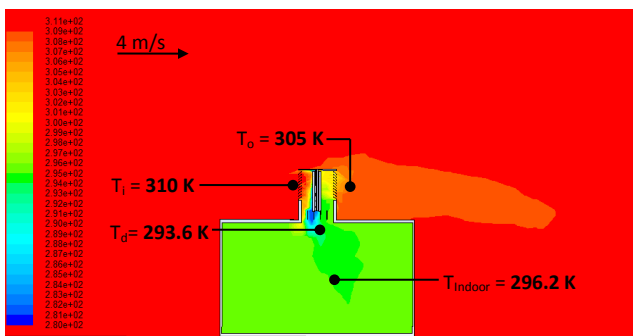


Figure 20 Temperature distributions inside the test room with a modern wind tower incorporating the vertical HTD arrangement

Figure 21 illustrates temperature distribution inside the test room integrated with a one-sided wind tower device with horizontal HTD arrangement.

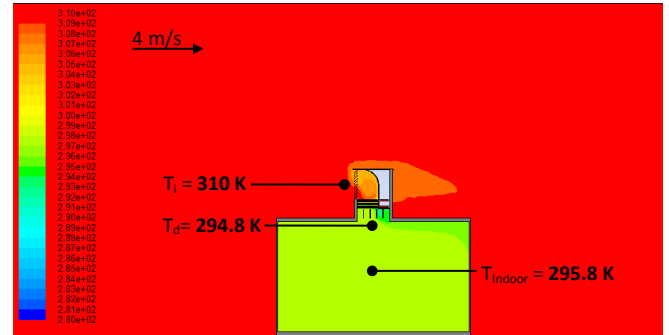


Figure 21 Temperature distributions inside the test room with a modern wind tower incorporating the horizontal HTD arrangement

5. DISCUSSION

Figure 10 shows the velocity contours inside the terminal of the tower with evaporative cooling and HTD. Sample points are created to measure the variation of air flow velocity and temperature from the inlet to the outlet. The result also highlighted the existence of separation zones and wake regions near the lower edge of the opening causes the variation of pressure coefficient at the tower's entrance. As a result, the wind tower could not achieve its maximum efficiency.

With reference to Figure 10a, computational air velocity of 5 m/s is obtained at the outlet of the geometry, which is 67 % higher than the set inlet speed. This is due to the increased negative buoyancy force. Figure 10b, shows the effect of the wind tower components (louvers, dampers and HTD) on the ventilation performance of the device, an average on 2.52 m/s is obtained at the tower outlet.

The CFD results (Figure 11 and 13) of the wind tower system incorporating evaporative cooling methods have been validated against research carried out by Kalantar [6] on a wind catcher by using both analytical and CFD analysis. A similar geometrical structure, boundary conditions and CFD codes were applied. Figure 11 shows the comparison between the air velocity obtained from the CFD results and literature. The velocity of the air inside the tower is plotted against the distance from inlet to outlet. It is observed that after spraying water in the air, the velocity increased rapidly due to the absorption of water by air and it is in a heavier state (increased negative buoyancy force). Good correlation between the different methods of analysis was observed.

Figure 12a displays the contours of static temperatures inside the traditional wind tower. An average temperature of 296K is obtained at the outlet of the device, with the inlet temperature set at 310 K. While the outlet temperature of the wind tower with HTD (Figure 12b) was reduced by up to 15 K.

Figure 13 shows the comparison between the airflow temperature CFD results and data obtained from the literature [6]. The static temperature at the cross-section of

the tower is plotted against the distance from inlet to outlet. It is observed that the temperature is significantly reduced after passing the evaporative cooling device. The temperature reduction is a result of the latent heat of the induced air that is absorbed by the water as it changes from liquid to vapor. It is seen that after spraying water in the air, the temperature decreased rapidly and slightly increased as it reaches the walls near the outlet of the tower which are not isolated against heat transfer. Good correlation between the different methods of analysis was observed (average of 0.05 % error).

The CFD study highlighted the effect of the wind tower vertical height on the thermal performance of the two types of wind tower cooling system. Figure 14 displays the variation of temperature of airflow from inlet to outlet. The cooling systems are capable of decreasing air temperatures by 13-15 K. Majority of the reductions for both models is achieved within the top of the tower (2 meters). A steady temperature drop is observed at the upper section of the evaporative cooling tower and stabilizes at 295 K as it approaches the outlet of the channel. The air temperature is slightly elevated as it moves towards the lower walls of the tower which is not isolated against heat transfer. While in the proposed model, the air temperature dropped rapidly from 310 to 293 K after passing the heat transfer devices. Similarly, small increase in temperature is observed at the lower section of the channel.

Figure 15 compares the effect of varying wind tower height on the exit air temperature. It can be seen that the traditional system is greatly dependent on the height of the tower, exit temperature increased up to 3.8 K after reducing the tower height by 8 m. While height is not a factor for the proposed heat transfer device arrangement, making it highly viable for modern roof-mounted wind tower systems.

Figure 16 is based on the front view of the geometry displaying the velocity contour plot. The velocity contour of the cross sectional planes in the test room model represents the air flow distribution within the structure. As seen from the illustration, the air is accelerated as it enters the opening of the one-sided wind tower. The air stream is circulated inside the structure and exits the opening located on the other end.

Figure 17 depicts the simulated temperature distribution inside the test room with a uni-directional wind tower incorporating the HTD arrangement. Temperature reduction of 12.6 K is obtained from the CFD analysis for external wind speeds 4 m/s.

Figure 18 illustrates the measurement points at 1.5 m height. Uneven airflow distribution is observed inside the structure, air flow velocity (point 5) of 0.7 m/s is obtained directly below the wind tower diffuser, which is about twice

the air stream velocity near the side walls. This is due to the dampers of the system set to 0° (fully open).

As depicted in Figure 19, the dynamic pressure contours for the standard row housing model is obtained with an average micro-climate pressure of 0.43 Pa. As seen from the diagram, the dynamic pressure inside the structure is significantly lower compared to the inlet conditions.

Figure 20 and 21 displays the contour of static temperatures inside the test room with a wind tower incorporating the vertical and horizontal HTD arrangement. Air temperature reduction is observed inside the microclimate, average temperature of 296.2 and 295.8 K are obtained inside the models for external wind speed of 4 m/s, which is 11-12 % lower, compared to the wind tower employing evaporative cooling devices.

6. CONCLUSIONS

A wind tower system incorporating heat transfer devices was designed to meet the internal comfort criteria in extreme conditions. Heat transfer devices were installed inside the passive terminal of the wind tower unit, highlighting the potential to achieve minimal restriction in the external air flow stream while ensuring maximum contact time, thus optimizing the cooling duty of the device. A numerical analysis was carried out using CFD software to simulate and analyze the air flow pattern, pressure coefficient and temperature distribution around and through the wind tower to the test room. The CFD results of the wind tower system incorporating evaporative cooling methods have been validated against data obtained from the literature. Good correlation between the different methods of analysis was observed. The work highlighted the effect of evaporative cooling and heat transfer devices on the thermal performance of the passive ventilation device. The proposed cooling system was capable of reducing the air temperatures by 12-15 K, depending on the configuration and operating conditions. The findings revealed that height was not a factor for the proposed heat transfer device arrangement, making it highly viable for modern roof-mounted wind tower systems. Furthermore, a standard four-sided wind tower system is utilized as a simulation benchmark model for the analysis and comparison of the ventilation and thermal performance of the proposed wind tower configurations. Results have indicated that the internal airflow rate was slightly reduced following the integration of the vertical and heat pipe configuration, reductions of 4.11 % and 8.21 % were obtained from the achieved computational model.

REFERENCE

1. Energy Efficiency in Buildings: Transforming the Market [Online], 2011, available from: www.wbcscd.org
2. Hughes B.R., Calautit J.K., Chaudhry H.N. Advancement of Natural Ventilation Technologies for Sustainable Development. The ESE2012 Symposium;2012, 71-84.

3. Hughes B.R. and Cheuk-Ming M. A Study of Wind and Buoyancy Driven Flows Through Commercial Wind Towers. *Building and Environment*; 2011, 43, 1784-1791.
4. Jones B. and Kirby R. Quantifying the performance of a top-down natural ventilation Windcatcher™. *Building and Environment*; 2008, 44, 1925-1934.
5. Hughes B.R., Calautit J.K., Ghani S.A. The Development of Commercial Wind Towers for Natural Ventilation: a review *Applied Energy*; 2012, 92, 606-627.
6. Kalantar V. Numerical simulation of cooling performance of wind tower (Baud-Geer) in hot and arid region. *Renewable Energy*; 2009, 34, 246–254.
7. Bouchahm Y., Bourbia F. and Belhamri A. Performance analysis and improvement of the use of wind tower in hot dry climate. *Renewable Energy*; 2011, 36, 898-906.
8. Badran A. Performance of cool towers under various climates in Jordan. *Energy and Buildings*; 2003, 35, 1031–1035.
9. Saffari H. and Hosseinnia S. Two-phase Euler-Lagrange CFD simulation of evaporative cooling in a Wind Tower. *Energy and Buildings*; 2009, 41, 991–1000.
10. Mehta U. Some aspects of uncertainty in computational fluid dynamics results. *Journal of Fluids Engineering*; 1991, 113, 539–543
11. Chung T. *Computational fluid dynamics*. Cambridge University Press, 2002, 1, 15-21.
12. Calautit J.K., Hughes B.R., Ghani S.A. A Numerical Investigation into the Feasibility of Integrating Green Building Technologies into Row Houses in the Middle East. *Architectural Science Review*; 2013, 56, 279-296.
13. Calautit J.K., Hughes B.R., Ghani S.A. Numerical Investigation of the Integration of Heat Transfer Devices into Wind Towers, *Chemical Engineering Transactions*; 2013, 34, 43-48.
14. Calautit J.K., Chaudhry H.N., Hughes B.R., Ghani S.A. Comparison between evaporative cooling and a heat pipe assisted thermal loop for a commercial wind tower in hot and dry climatic conditions, *Applied Energy*; 2013, 101, 740-755.